Monooxygenase Activity of Type 3 Copper Proteins

SHINOBU ITOH*,† AND SHUNICHI FUKUZUMI‡

Department of Chemistry, Graduate School of Science, Osaka City University, 3-3-138 Sugimoto, Sumiyoshi-ku, Osaka 558-8585, Japan, and Department of Material and Life Science, Graduate School of Engineering, Osaka University, SORST, Japan Science and Technology Agency (JST), 2-1 Yamada-oka, Suita, Osaka 565-0871, Japan

Received December 7, 2006

ABSTRACT

The molecular mechanism of the monooxygenase (phenolase) activity of type 3 copper proteins has been examined in detail both in the model systems and in the enzymatic systems. The reaction of a side-on peroxo dicopper(II) model compound (**A**) and neutral phenols proceeds via a proton-coupled electron-transfer (PCET) mechanism to generate phenoxyl radical species, which collapse each other to give the corresponding C–C coupling dimer products. In this reaction, a bis(μ-oxo)dicopper(III) complex (**B**) generated by O–O bond homolysis of **A** is suggested to be a real active species. On the other hand, the reaction of lithium phenolates (deprotonated form of phenols) with the same side-on peroxo dicopper(II) complex proceeds via an electrophilic aromatic substitution mechanism to give the oxygenated products (catechols). The mechanistic difference between these two systems has been discussed on the basis of the Marcus theory of electron transfer and Hammett analysis. Mechanistic details of the monooxygenase activity of tyrosinase have also been examined using a simplified enzymatic reaction system to demonstrate that the enzymatic reaction mechanism is virtually the same as that of the model reaction, that is, an electrophilic aromatic substitution mechanism. In addition, the monooxygenase activity of the oxygen carrier protein hemocyanin has been explored for the first time by employing urea as an additive in the reaction system. In this case as well, the ortho-hydroxylation of phenols to catechols has been demonstrated to involve the same ionic mechanism.

Introduction

Tyrosinase (EC 1.14.18.1), catechol oxidase (EC 1.10.3.1), and hemocyanin are the members of the type 3 copper protein family involving a magnetically coupled dinuclear copper reaction center.[1,2] Each copper ion is ligated by three histidine imidazoles, holding molecular oxygen in a side-on binding mode to give a (μ-η^2:η^2-peroxo)dicopper(II) complex (**A**) as the common active-oxygen species

Chart 1

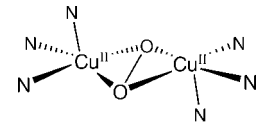

A

Scheme 1

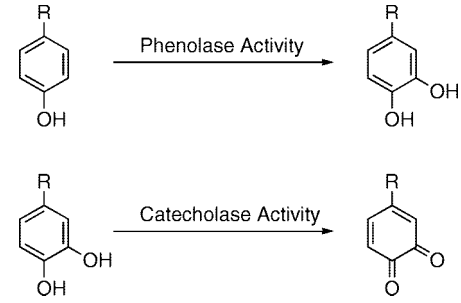

(Chart 1).[3–5] In spite of having the same side-on peroxo dinuclear copper(II) species, however, these copper proteins exhibit different chemical reactivity toward exogenous substrates. Namely, tyrosinase catalyzes ortho-hydroxylation of phenols to the corresponding catechols, so-called phenolase activity, as well as dehydrogenation of catechols to the corresponding *o*-quinones, which is called catecholase activity (Scheme 1).[1,2] *o*-Quinone formation from tyrosine is the initial step for the synthesis of melanin pigments in nature.[6] On the other hand, catechol oxidase exhibits only catecholase activity without showing the monooxygenase activity.[4] Furthermore, hemocyanin has only the reversible dioxygen binding ability, thus acting as the oxygen storage and carrier protein of mollusks and arthropods.[1,2,5] These differences in the chemical reactivity among the type 3 copper proteins can be attributed to the different architectures of the enzyme active sites as in the case of heme proteins which dictate a wide variety of functions at similar iron–porphyrin reaction centers.[7] The chemical reactivity of the metalloproteins is thereby controlled by the arrangement of amino acid side chains in the active sites.

Scheme 2 shows a proposed catalytic mechanism of tyrosinase. The native enzymatic reaction involves many fundamental catalytic steps such as binding of dioxygen to deoxy-tyrosinase [dicopper(I) form] to generate peroxo species **A** (oxy-tyrosinase) (path a), association of the substrate with oxy-tyrosinase (paths b and e), oxygen atom transfer from **A** to the substrate to give catecholate product (path c), and dehydrogenation of catechol to *o*-quinone (paths d, f, and g).[8] Among these processes, the oxygenation of phenols by the peroxo species (path c) is most attractive from the viewpoints of synthetic organic chemistry and catalytic oxidation chemistry. However, the mechanism of the oxygen atom-transfer process has yet to be fully clarified due to the complicated side reactions

Shinobu Itoh received his Doctor's degree in engineering from Osaka University in 1986. Then, he joined the Department of Applied Chemistry of Osaka University as an Assistant Professor (1986–1994) and an Associate Professor (1994–1999). During that period, he spent a year (1987–1988) as a postdoctoral fellow in Professor Teddy G. Traylor's group at the University of California, San Diego (La Jolla, CA). In 1999, he moved to Osaka City University as a Professor. His current research interest is chemical modeling and application of redox active sites in biological systems.

Shunichi Fukuzumi received his Ph. D degree from Tokyo Institute of Technology (Tokyo, Japan) in 1978. He did postdoctoral work with Professor Jay K. Kochi at Indiana University (Bloomington, IN) from 1978 to 1981. After that, he joined the Department of Applied Chemistry of Osaka University and became a Professor in 1994. His research interest is centered on mechanisms and catalysis in electron-transfer chemistry of various organic compounds, organometallic compounds, and metal complexes.

* To whom correspondence should be addressed. E-mail: shinobu@sci.osaka-cu.ac.jp.

† Osaka City University.

‡ Osaka University.

10.1021/ar6000395 CCC: $37.00
Published on Web 04/27/2007

Scheme 2

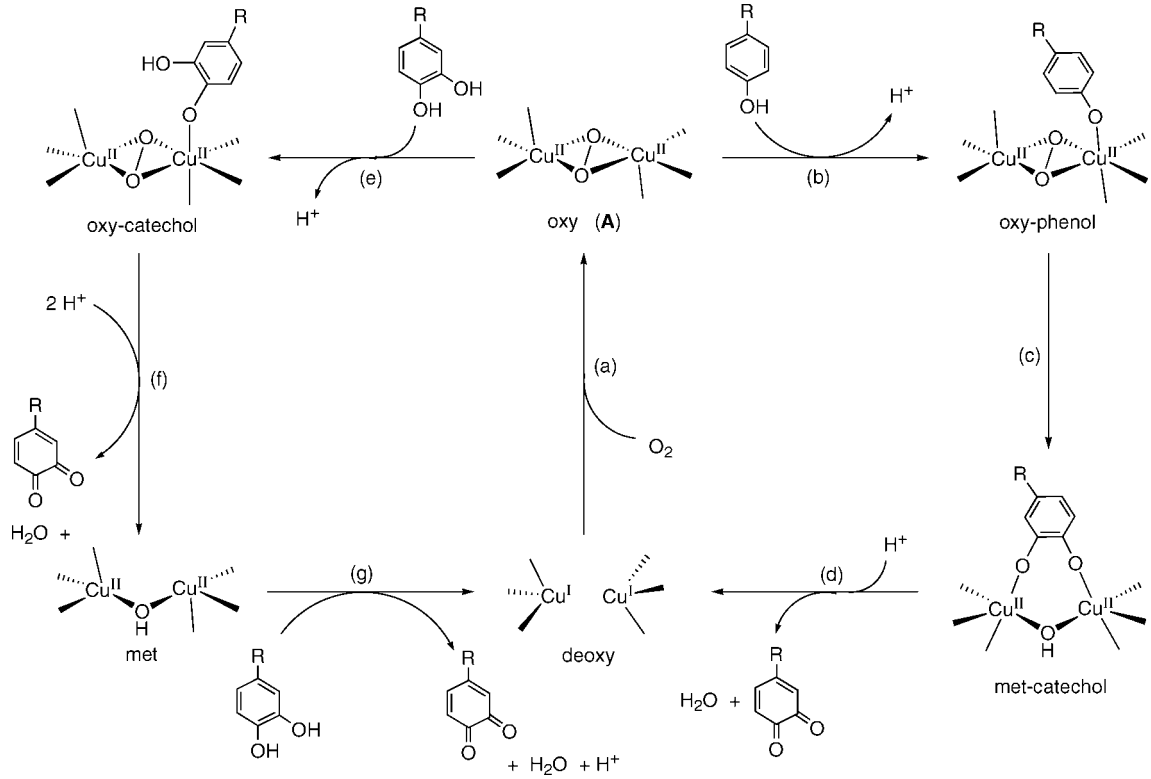

such as nonenzymatic transformation of the *o*-quinone products to melanin pigments.[6] Moreover, such side reactions have precluded adaptation of the enzymatic reaction (oxygenation of phenols to catechols) to synthetic organic chemistry.

In this Account, we summarize our recent research activity aiming at understanding the mechanistic details of phenolase activity of tyrosinase (path c) both in the model systems and in the enzymatic systems. Development of a simplified catalytic system of tyrosinase by prohibiting the melanin pigment formation process (side reactions) has enabled us to perform direct comparison of the mechanisms between the model reaction and the enzymatic reaction. This provided profound insights into the molecular mechanism of dioxygen activation chemistry at the dinuclear copper reaction centers. Furthermore, the monooxygenase activity of oxygen carrier protein hemocyanin has been evaluated for the first time to demonstrate that a small perturbation of the protein matrix triggers the induction of different chemical functions of the type 3 copper proteins.

Model Reactions

One of the greatest successes in bioinorganic chemistry is the correct prediction of the active-oxygen species of tyrosinase and hemocyanin by using simple model compounds.[1,2,9,10] Kitajima and his co-workers reported the first crystal structure of the side-on peroxo dicopper(II) complex (**A**) supported by hydrotris(pyrazolyl)borate ligands.[9] The spectroscopic features of the model complexes matched well those of oxy-hemocyanin, strongly suggesting the same side-on binding mode of the peroxo

Scheme 3

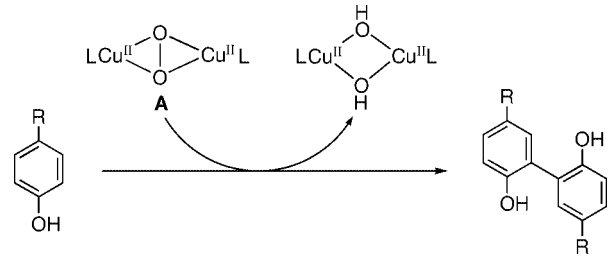

ligand in the proteins.[9,10] This was confirmed in 1994 by the X-ray structural determination of oxy-hemocyanin almost 5 years after the discovery of **A** in the model systems.[5a] So far, the (μ-η^2:η^2-peroxo)copper(II) complexes supported by a variety of tridentate N_3 and bidentate N_2 ligands have been reported to provide important information about the effects of the ligand on the structure and physicochemical properties of the peroxo complexes.[11–14]

C–C Coupling Reaction of Phenols. Reactions of the peroxo complexes **A** and phenol derivatives have widely been investigated in the model systems to gain insight into the catalytic mechanism of tyrosinase.[12,15,16] In most cases, however, the reaction of **A** and neutral phenols afforded C–C coupling dimer products (Scheme 3) rather than the oxygenation product catechols.[12,15,16] The results clearly indicate that the reactions of neutral phenols and the peroxo complex **A** involve phenolic O–H bond activation generating phenoxyl radical intermediates. The generated phenoxyl radical species spontaneously collapse each other to give the C–C coupling dimer products. Then, an important question arises; what is the major factor controlling the reaction pathways between catechol for-

Chart 2

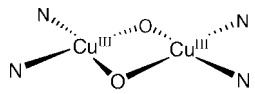

B

Chart 3

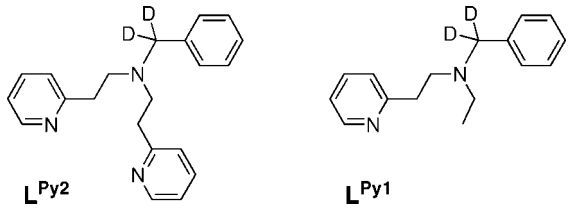

L^{Py2} L^{Py1}

mation (Scheme 1) and the C–C coupling reaction (Scheme 3)?

To address this issue, we have also investigated the reactions of phenols with a (μ-η^2:η^2-peroxo)copper(II) complex (**A**) supported by tridentate ligand L^{Py2} and also with a bis(μ-oxo)dicopper(III) complex (**B** in Chart 2) prepared by using bidentate ligand L^{Py1}.[16] To protect the ligands from oxidative N-dealkylation of the ligand side arm by the Cu_2O_2 species, the benzylic position of the ligands is deuterated as shown in Chart 3.[17,18]

Treatment of para-substituted phenols *p*-X-C_6H_4OH with the peroxo complex **A** supported by L^{Py2} at −80 °C under anaerobic conditions gave the corresponding C–C coupling dimer in ∼50% yields based on peroxo complex **A**.[16] This result clearly indicates that peroxo complex **A** formally acts as a one-electron oxidant for ArOH to produce an equimolar amount of $ArO^{\bullet}$, which spontaneously dimerizes to give the C–C coupling dimer product in nearly 50% yields based on **A**. Figure 1 shows the plots of log k^A_2 (the second-order rate constant for the C–C coupling reaction) against the E^0_{ox} values of the phenol substrates.[16]

The log k^A_2 values increase with an increase in driving force of electron transfer from phenols to **A**, i.e., with a decrease in the E°_{ox} values (Figure 1). According to the Marcus theory of electron transfer [$\log k = \log Z - (F/2.3RT)(E^{\circ}_{ox} - E^{\circ}_{red})$], a plot of log *k* versus the free energy change of electron transfer (ΔG°_{et}), which is given by $F(E^{\circ}_{ox} - E^{\circ}_{red})$, should be linear with a slope of −26.1 at −80 °C, provided that the driving force of electron transfer ($-\Delta G^{\circ}_{et}$) is much smaller than the reorganization energy of electron transfer (λ).[19] A plot of log k^A_2 versus E°_{ox} for the one-electron oxidation of phenols by **A** afforded a good linear correlation as expected for an electron transfer reaction (part A in Figure 1).[16] However, the absolute value of the negative slope of the experimental data (−18.8 at −80 °C) was somewhat smaller than that of the theoretical value (−26.1 at −80 °C).[16]

The electron transfer from ArOH to **A** may be followed by proton transfer from the resulting cation radical intermediate $ArOH^{\bullet+}$ to an intermediate **D** $[Cu_2/O_2]^+$ to generate a phenoxyl radical $ArO^{\bullet}$ and the product complex **E** $[Cu_2/O(OH)]^{2+}$ (Scheme 4). Intermediate **D** is either a (μ-oxo)(μ-oxyl radical)dicopper(II) or a bis(μ-oxo)dicopper(II,III). The phenoxyl radicals $ArO^{\bullet}$ thus produced may readily collapse each other to give the C–C coupling dimer product in ∼50% yield based on **A** as experimentally observed.

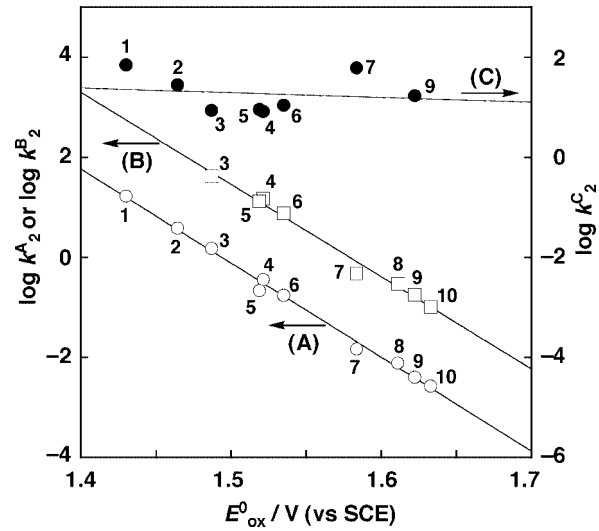

FIGURE 1. Plots of log k^A_2, log k^B_2, and log k^C_2 against the oxidation potentials (E°_{ox}) of ArOH (**1**, 4-$MeOC_6H_4OH$; **2**, 2,4-^{t}BuC_6H_3OH; **3**, 4-$PhOC_6H_4OH$; **4**, 4-PhC_6H_4OH; **5**, 4-^{t}BuC_6H_4OH; **6**, 4-MeC_6H_4OH; **7**, 2,4,6-^{t}BuC_6H_2OH; **8**, 4-FC_6H_4OH; **9**, 2,6-^{t}BuC_6H_3OH; **10**, 4-ClC_6H_4OH) for the reactions of ArOH with (μ-η^2:η^2-peroxo)dicopper(II) complex (**A**), bis(μ-oxo)dicopper(III) complex (**B**), and cumylperoxyl radical (**C**) in acetone at −80 °C. Reproduced from ref 16. Copyright 2003 American Chemical Society.

Scheme 4

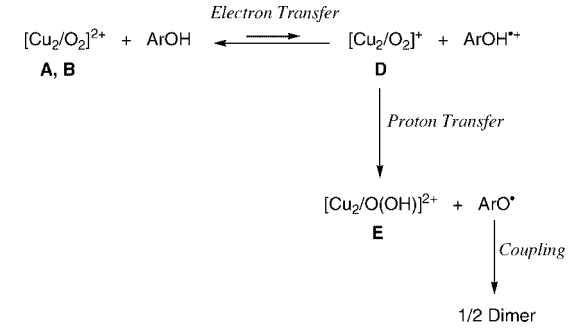

If the electron transfer from phenols to the peroxo complex **A** in Scheme 4 were the rate-determining step, followed by a fast proton-transfer step, the slope of the Marcus plot in Figure 1 (part A) would be close to the theoretical value of −26.1, when the electron transfer is exergonic (when the free energy change of electron transfer is negative).[19] Thus, the smaller negative slope of −18.8 observed in Figure 1 (part A) suggests that the electron transfer from phenols to **A** is endergonic and coupled with the proton transfer (PCET) as shown in Scheme 4. This is supported by the observed kinetic deuterium isotope effects on the second-order rate constants k^A_2 [$k^A_{2(H)}/k^A_{2(D)}$ = 1.2–1.6 depending on the substrates].[16] The distinct kinetic deuterium isotope effects (1.2–1.6) clearly indicate that the electron transfer is indeed coupled with proton transfer via a concerted mechanism rather than a two-step mechanism. The $k^A_{2(H)}/k^A_{2(D)}$ values are significantly smaller than the

Scheme 5

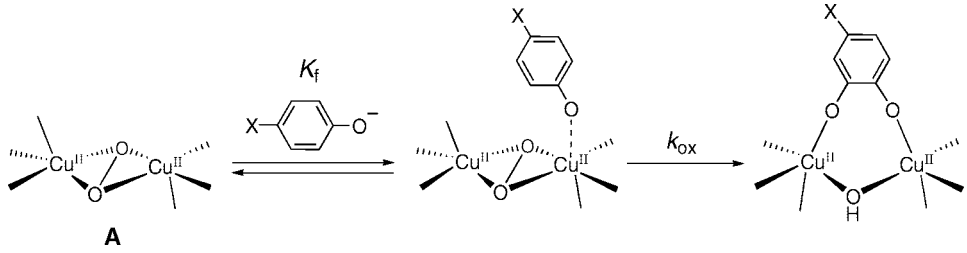

kinetic deuterium isotope effects observed in the hydrogen atom-transfer reaction (HAT) from toluene and dihydroanthracene to permanganate ($k_H/k_D = 6 \pm 1$ and 3.0 $\pm$ 0.6, respectively)[20] but are nearly the same as that reported for the concerted PCET reaction between guanine and $Ru(bpy)_3^{3+}$ ($k_H/k_D = 1.4$).[21] DFT studies by Mayer and co-workers have also suggested that the concerted PCET mechanism is more likely than the HAT mechanism for the oxidation of a phenol to a phenoxyl radical species.[22]

Oxidation of phenols by the bis(μ-oxo)dicopper(III) complex **B** supported by L^{Py1} also proceeded under the same experimental conditions to give the same C–C coupling dimer product in nearly 50% yield.[16] A plot of log k^B_2 versus $E°_{ox}$ for the oxidation of phenols by **B** in Figure 1 (part B) also gave a good linear correlation with virtually the same slope (−18.4) as that in the case of **A**. Furthermore, kinetic deuterium isotope effect values [$k^B_{2(H)}/k^B_{2(D)} = 1.2–1.5$] were also nearly the same as those of the reactions with **A**. These results clearly indicate that electron transfer from phenols to **B** is also coupled with the subsequent proton transfer (PCET) as in the case of **A** (Scheme 4).

Cumylperoxyl radical $Ph(CH_3)_2COO^•$ (**C**) has been demonstrated to act as a hydrogen atom acceptor in the reaction with *N*,*N*-dimethylanilines, where a one-step hydrogen atom-transfer (HAT) mechanism has been confirmed.[23] In the reactions of the same series of phenols with **C**, however, the log k^C_2 values are rather constant irrespective of the $E°_{ox}$ values (slope = −0.95) as shown in Figure 1 (part C). The weak rate dependence of log k^C_2 on $E°_{ox}$ is similar to the case of the HAT reaction with *N*,*N*-dimethylanilines.[23] The contrasting results in Figure 1 (parts A and B vs part C) confirm that the electron-transfer step is definitely involved in the oxidation of phenols by the (μ-η^2:η^2-peroxo)dicopper(II) complex (**A**) and the bis(μ-oxo)dicopper(III) complex (**B**).

The identical slope of the log k_2 versus $E°_{ox}$ plots between the reactions of **A** and **B** suggests that a common active-oxygen species is involved in these reactions. In such a case, bis(μ-oxo)dicopper(III) complex **B** may be the actual active species, and the rate difference between the two systems can be attributed to the difference in the absolute concentration of **B**. Although the peroxo complex **A** is the major species in the tridentate ligand system L^{Py2}, the actual reactive species bis(μ-oxo) complex **B** may exist as a minor component in the rapid equilibrium between them. This is consistent with the previous report that the bis(μ-oxo)dicopper(III) complex **B** coexists as a minor

Table 1. Formation Constants (K_f) and Rate Constants (k_{ox}) for the Reactions between $[Cu^{II}_2(L^{Py2})_2(\mu\text{-}O_2)](PF_6)_2$ and *p*-X-C_6H_4OLi in Acetone at −94 °C

X	K_f (M^{-1})	k_{ox} (s^{-1})
^{t}Bu	–[a]	–[a]
Me	–[a]	–[a]
Br	465	0.93
Cl	570	0.76
F	948	0.63
COMe	493	0.086
COOMe	940	0.083

[a] Too fast to be determined accurately.

product when the (μ-η^2:η^2-peroxo)dicopper(II) complex is prepared using 2-(2-pyridyl)ethylamine tridentate ligands [$(PyCH_2CH_2)_2NR$].[24]

Oxygenation of Phenolates to Catechols. In contrast to the reaction of neutral phenols with the side-on peroxo dicopper(II) complex **A**, the reaction of phenolates (deprotonated form of phenols) with **A** gave the oxygenated product (catechols), where neither the corresponding *o*-quinone derivative nor the C–C or C–O coupling dimer was obtained.[25,26] For example, the reactions of lithium phenolates with various para substituents (X = ^{t}Bu, Me, Br, Cl, F, COMe, or COOMe) and the (μ-η^2:η^2-peroxo)dicopper(II) complex (**A**) supported by L^{Py2} gave the corresponding catechols in fairly good yields (60–99%).[26] The isotope labeling experiments using $^{18}O_2$ have confirmed that the origin of the incorporated oxygen atom of the catechol product is molecular oxygen.[26] In contrast to such efficient catechol formation with the peroxo complex **A**, no catechol was formed when a bis(μ-oxo)dicopper(III) complex **B** supported by L^{Py1} was employed under the same experimental conditions.[26]

The reaction rate was first-order with respect to the concentration of the peroxo complex **A**, and a plot of the observed first-order rate constant k_{obs} versus the substrate concentration afforded a Michaelis–Menten type saturation curve.[26] This can be attributed to formation of a complex between the substrate and the peroxo species **A** prior to the oxygen atom-transfer reaction as illustrated in Scheme 5.

The reactivity of the substrates increases with an improvement in the electron donating ability of the para substituent as seen in Table 1. Notably, a plot of log k_{ox} versus $E°_{ox}$ (the one-electron oxidation potentials of lithium phenolates) afforded a linear correlation with a small negative slope of −2.8 at −94 °C. The absolute value of the slope is significantly smaller than that (−18.8) of a

Scheme 6

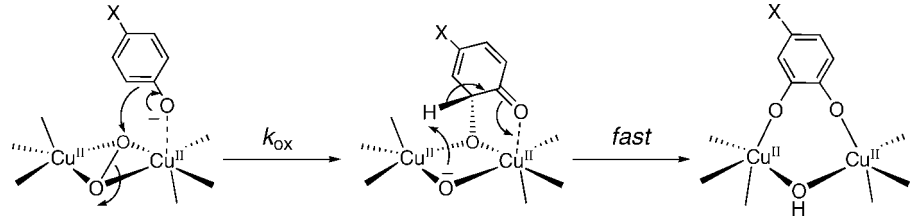

Scheme 7

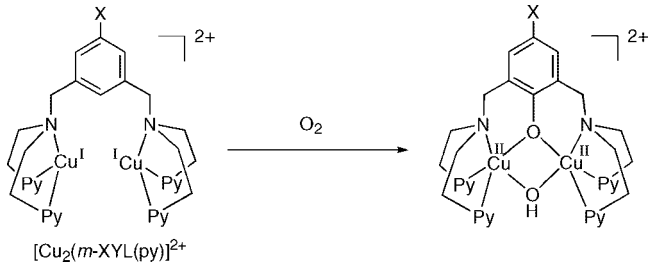

Scheme 8

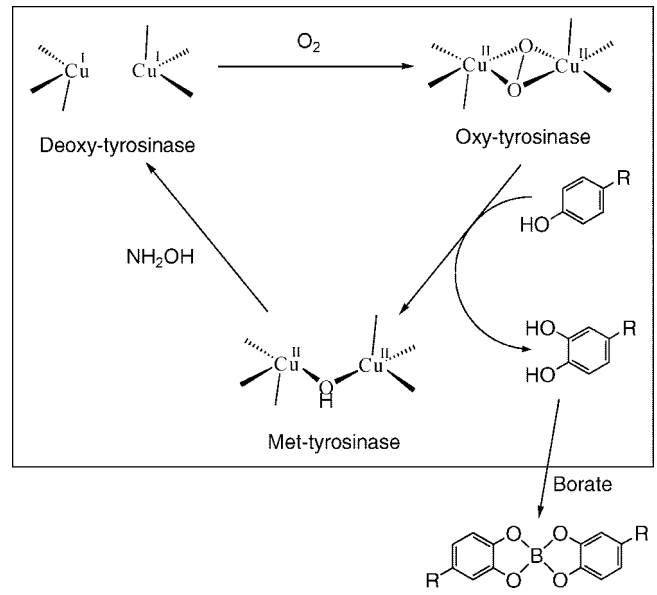

similar plot (log k^{A}_{2} vs E°_{ox}) for the C–C coupling reaction of neutral phenols involving an electron-transfer step (Figure 1, part A). The value is, on the other hand, larger than that (−0.95) of the HAT reaction of phenols with cumylperoxyl radical (**C**) (Figure 1, part C). These results may suggest that the oxygenation reaction of phenolate by the side-on peroxo complex **A** involves neither electron transfer nor hydrogen atom transfer but proceeds via an ionic mechanism such as an electrophilic aromatic substitution mechanism as illustrated in Scheme 6. In this case, the C–O bond formation (the first process in Scheme 6) is the rate-determining step, and the subsequent proton migration from the generated intermediate (the second process) is much faster, since there was no kinetic deuterium isotope effect, when *p*-Cl-C_6D_4OLi was used instead of *p*-Cl-C_6H_4OLi ($k_{ox}{}^{H}/k_{ox}{}^{D} = 1.0 \pm 0.1$).[26]

The electrophilic aromatic substitution mechanism in Scheme 6 was further supported by the Hammett analysis (plot of log k_{obs} vs Hammett constant σ^{+}), which gave a negative slope (Hammett ρ value) of −1.8.[26] This value is fairly close to the ρ value (−2.1) of the aromatic ligand hydroxylation reaction of a (μ-η^2:η^2-peroxo)dicopper(II) complex (**A**) in a dinuclear copper model system shown in Scheme 7.[27] Karlin and co-workers unambiguously demonstrated that the aromatic ligand hydroxylation involves the electrophilic aromatic substitution mechanism.[27]

As has been demonstrated above, the oxidation of neutral phenol by the Cu_2–O_2 complexes (**A** and **B**) proceeds via a PCET mechanism, whereas the oxygenation of phenolates by **A** involves an ionic mechanism (electrophilic aromatic substitution mechanism). Moreover, the reaction of the phenolates and **B** produced neither the C–C coupling dimer nor the oxygenation product (catechol). These results indicate that the one-electron reduction potentials (E°_{red}) of **A** and **B** are lower than the one-electron oxidation potentials (E°_{ox}) of phenol(ate)s, even though the accurate values of E°_{red} have yet to be determined. In the oxidation of neutral phenols, the initial electron transfer from the phenol substrates to Cu_2–O_2 complexes may be energetically uphill, whereas the subsequent proton transfer to generate the phenoxyl radical may be highly downhill in rendering the overall reaction to completion. In the case of phenolate substrates, the electron transfer from the phenolate to the Cu_2–O_2 complexes may also be uphill to prohibit formation of the phenoxyl radical, whereas the anionic reaction (electrophilic aromatic substitution reaction) proceeds much faster to oxygenate phenolates to catechols as illustrated in Scheme 6. This may be the reason why neutral phenols afforded the C–C coupling dimer whereas phenolate substrates gave the oxygenation products, catechols.

Monooxygenase Mechanism of Tyrosinase

Little had been known about the mechanistic details of the monooxygenase (phenolase) activity of tyrosinase, since the enzymatic reaction is very complicated involving many fundamental catalytic processes (paths a–g in Scheme 2) and is blinded by significant side reactions such as nonenzymatic transformation of *o*-quinone products to melanin pigments.[6] To overcome such problems, we have recently developed a simplified catalytic system of mushroom tyrosinase using a borate buffer as the reaction medium and NH_2OH as the sacrificial reductant (Scheme 8).[28] In this system, borate anion of the buffer solution forms a stable complex with the primary oxygenation product catechol[29] to prevent its overoxidation to *o*-

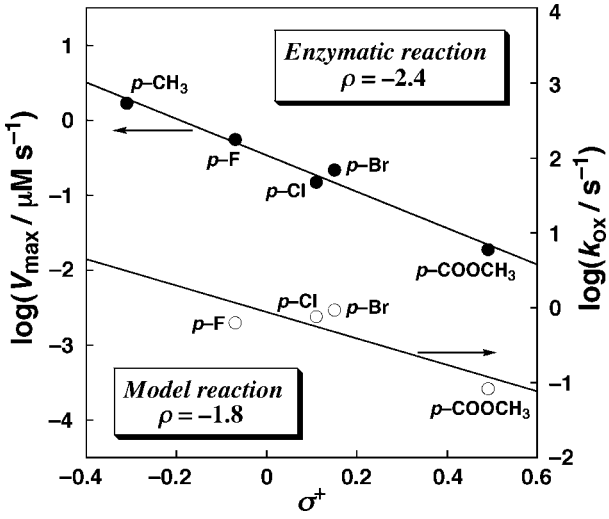

FIGURE 2. Plots of log V_{max} [enzymatic reactions (●)] and log k_{ox} [model reactions (○)] vs Hammett constants σ^+ of the para substituents. Reproduced from ref 28. Copyright 2003 American Chemical Society.

quinone (paths d, e, and g in Scheme 2). This eventually prohibits melanin pigment formation to simplify the catalytic cycle significantly.[28] In this case, however, no reduction of met-tyrosinase [hydroxo-bridged dicopper(II) resting state] to deoxy-tyrosinase [dicopper(I) form] (paths d and g) proceeds because a native electron donor (catechol) is absent due to the formation of the complex with borate anion as mentioned above.[28] Thus, NH_2OH was added as an external reductant to reconstruct the reduction process from met-tyrosinase to deoxy-tyrosinase.[28] By using this simplified catalytic system, we have succeeded in examining the oxygen atom-transfer process from peroxo intermediate **A** to the phenol substrates (path c) without the interference by the side reactions.[28]

The catalytic reaction was followed by monitoring the O_2 consumption rate (v_{app}) using an ordinary O_2 electrode to exhibit a Michaelis–Menten type saturation dependence of v_{app} on the substrate concentration.[28] Then, the kinetic parameters (K_M and V_{max}) for several para-substituted phenols were determined, and the log V_{max} values of the enzymatic reaction are plotted against Hammett σ^+ together with the log k_{ox} values of the model reactions (Figure 2).[28]

The log V_{max} values of the enzymatic reactions increase as the electron donor ability of the para substituents of the substrates increases (Figure 2). This clearly indicates that the peroxo intermediate of oxy-tyrosinase exhibits an electrophilic nature as in the case of the model systems.[26,27] More importantly, the ρ value of the Hammett plot of the enzymatic reaction (−2.4) is fairly close to that of the model reaction (−1.8) (Figure 2).[26] Such a good agreement of the Hammett ρ values between the enzymatic and model reactions demonstrates clearly that the phenolase reaction of tyrosinase proceeds via the same mechanism as the model reactions, that is, an electrophilic aromatic substitution mechanism (Scheme 6).[28]

Although the crystal structure of mushroom tyrosinase is not yet available, the X-ray structure of bacterial

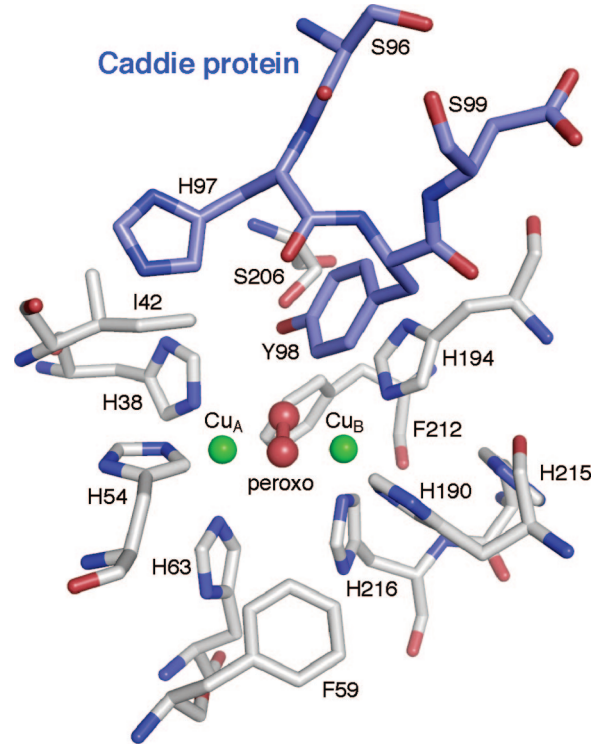

FIGURE 3. Active site structure of bacterial tyrosinase from *S. castaneoglobisporus*. Oxy form with caddie protein ORF378 (colored blue) (PDB entry 1WX4).[3a]

tyrosinase from *Streptomyces castaneoglobisporus*[3a] reported by Sugiyama and co-workers gives us valuable insight into the enzymatic reaction.[3b] Figure 3 shows the active site structure of oxy-tyrosinase with a caddie protein ORF378 (colored blue) which assists in the transportation of two Cu(II) ions into the tyrosinase catalytic center.[3a]

As clearly seen in Figure 3, there is a large space for substrate binding just above the Cu_2–O_2 core, which is occupied by caddie protein ORF378 in the crystal.[3a] Interestingly, a tyrosine residue (Tyr98) from the associated caddie protein extends into the active site pocket of tyrosinase, suggesting a similar orientation of bound substrate.[3a] In this case, the phenol moiety of Tyr98 is not hydroxylated since its hydroxyl group is more than 3.4 Å from the Cu_2O_2 unit, and a closer approach to the active site is prevented by the attachment to the caddie protein.[3a] This suggests that direct coordination of the substrate to the copper ion is prerequisite for the monooxygenation reaction as demonstrated by the model studies (Scheme 6).[26] In other words, the enzymatic reaction involves an ionic mechanism (electrophilic aromatic substitution mechanism) rather than a PCET mechanism which does not require direct coordination of phenols to copper of **A**. One of the histidine ligands for copper may act as a base to accept protons dissociated from the coordinated substrate as suggested by Sugiyama and his co-workers in their crystallographic studies on tyrosinase.[3a] They suggested that His54, which has a flexibility of geometry, is the most plausible candidate for that.[3a,30]

Monooxygenase Activity of Hemocyanin

The oxygen carrier protein hemocyanin is a large multisubunit protein whose structure varies significantly depending on the source of the protein.[31,32] Arthropod hemocyanin subunits have an M of ~75 kDa and associate into oligomers of hexamers in vivo.[31–33] On the other hand, molluskan hemocyanin subunits contain seven or eight oxygen-binding sites, termed functional units, having an M of ~400 kDa, which associate in multiples of 10 to yield cylindrical supramolecular assemblies.[31,32,34] Each subunit (functional unit) involves a type 3 copper center where O_2 is bound as a side-on peroxo form.[5] In contrast to tyrosinase and catechol oxidase, hemocyanin itself exhibits no redox reactivity toward external substrates in spite of having the same side-on peroxo dicopper(II) species (**A**).[1,2,8]

In this context, arthropod hemocyanins have recently been demonstrated to exhibit catecholase activity (Scheme 1), when they are treated with $NaClO_4$,[35] hydrolytic enzyme (trypsin or chymotrypsin),[36,37] or an antimicrobial peptide.[38] In these cases, conformational changes and/or partial hydrolysis of the protein may occur to open the active site pocket, allowing incorporation of substrate. However, mechanistic details about the enzymatic functions of arthropod hemocyanins have yet to be addressed. The redox reactivity of molluskan hemocyanin has been investigated even less thoroughly.[39]

We have recently found that molluskan hemocyanin from *Octopus vulgaris* exhibits phenolase (monooxygenase) activity toward phenol substrates, when it is treated with a typical denaturant urea.[40] The peroxo speceis **A** of oxy-hemocyanin, which is stable in the presence of a high concentration of urea (8 M) under anaerobic conditions (Ar) at 25 °C, readily reacts with phenols to give the corrresponding catechols (oxygenated product) in a 0.5 M borate buffer solution.[40] In the absence of urea, the reaction proceeds much slower.[40] In this case, the reaction could be followed by monitoring the decay of peroxo species **A** as shown in Figure 4, and the reactivities of variously para-substituted phenols were kinetically examined as in the case of tyrosinase system. The plot of log k_{app} vs the Hammett σ^+ gave a linear correlation, from which a Hammett ρ value was determined (−2.0). Notably, this value is very close to the Hammett ρ value of the phenolase reaction of mushroom tyrosinase (−2.4).[40] This indicates that the oxygenation of phenols by oxy-hemocyanin involves the same mechanism as the phenolase reaction of tyrosinase, that is, an electrophilic aromatic substitution mechanism. This mechasnim is consistent with the absence of a kinetic deuterium isotope effect [$k_{app(H)}/k_{app(D)} = 1.0$] with deuterated substrate p-ClC_6D_4OH.[40]

In contrast to the active site of tyrosinase (Figure 3), there is not enough space for substrate binding in the active site of octopus hemocyanin (Figure 5).[5c] In addition to the six His residues (copper ligands), Phe2567, Phe2698, Leu2830, and Thr2692 cover the Cu_2O_2 core of oxy-hemocyanin. Added urea may induce a conformational change in the protein matrix to move some of the amino acid residues away, allowing the substrate approach and binding.[41]

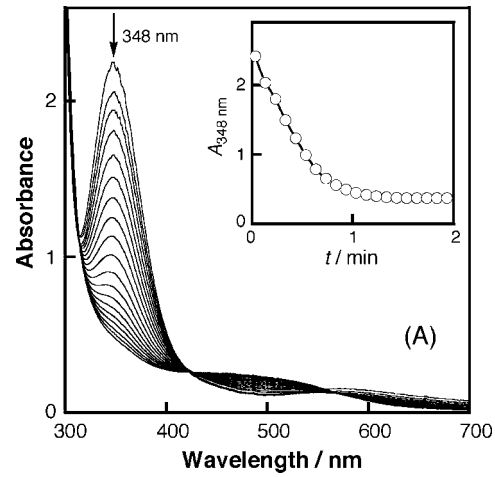

FIGURE 4. Spectral change observed upon addition of *p*-cresol (16 mM) to *Octopus* hemocyanin (0.17 mM) in 0.5 M borate buffer (pH 9.0) containing 10% MeOH and 8 M urea at 25 °C under Ar. The inset shows the time course of the absorption change at 348 nm. Reproduced from ref 40. Copyright 2006 American Chemical Society.

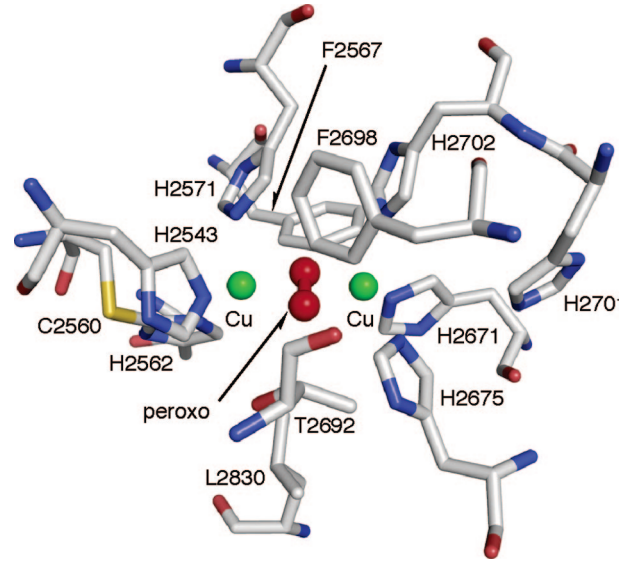

FIGURE 5. Active site structure of the Odg functional unit of oxy-hemocyanin from *Octopus dofleini* (PDB entry 1JS8).[5c]

Concluding Remarks

The ortho-hydroxylation reaction of phenols to catechols by (μ-η^2:η^2-peroxo)dicopper(II) complex **A** has been investigated in detail both in the model system and in the native enzymatic system.[16,26,28,40] It has been demonstrated that, in both systems, coordination of phenolic oxygen to one of the copper ions of the Cu_2O_2 core is essential for inducing the transfer of the oxygen atom from the peroxo complex **A** to the substrate via an electrophilic aromatic substitution mechanism. In the model system, however, coordination of neutral phenols to the copper ion of **A** may not occur due to the weak nucleophilicity

of the phenol oxygen. Thus, proton-coupled electron transfer (PCET) from the phenol to peroxo species **A** occurs mainly to give phenoxyl radical species, thus affording the C–C coupling dimer products.[15,16] Once the phenolic proton is removed to give phenolate, the coordinative interaction of the substrate to copper becomes possible for induction of formation of the C–O bond between the peroxo ligand and the ortho carbon of the substrate.[26] No phenoxyl radical formation is observed in the reaction of phenolates, probably because the oxidation potentials of phenolates ($E°_{ox}$) are higer than the reduction potential of **A** ($E°_{red}$).

In the active sites of tyrosianse and hemocyanin (Figures 3 and 5), there seems to be no specific amino acid residue which can act as a base to abstract a proton from the phenol substrate. Nonetheless, hydrophobic and/or $\pi-\pi$ stacking interactions may help incorporation of the phenol substrate to enhance its coordination of phenolic oxygen to copper ion. In such a case, a released proton may be accepted by one of the imidazole residues of the copper ligands.[3,30,42]

Recently, Stack and co-workers demonstrated in their model system that the coordination of phenolate to the copper ion of (μ-η^2:η^2-peroxo)dicopper(II) complex **A** induced homolytic cleavage of the O–O bond to give a bis(μ-oxo)dicopper(III) species **B**, which may act as a real active-oxygen species for the ortho-hydroxylation reaction.[43] They suggested that the C–O bond formation process between the phenolate substrate and **B** also involved an electrophilic ionic mechanism.[43] It should be noted, however, that the reaction of phenolate and the bis(μ-oxo) species **B** itself generated by using ligand L^{Py1} did not result in the oxygenation reaction at all.[26] The bis(μ-oxo)dinickel(III) complex generated by using Karlin's *m*-XYL(py) ligand (see Scheme 7) did not afford the aromatic ligand hydroxylation reaction, either.[44] This shows a sharp contrast to the (μ-η^2:η^2-peroxo)dicopper(II) system supported by the same ligand (see Scheme 7). Moreover, the DFT calculation studies on the tyrosinase reaction have demonstrated that the cleavage of the O–O bond of the side-on peroxo ligand of **A** in the enzymatic system is very endothermic by 23 kcal/mol.[45] This result ruled out the possible contribution of **B** in the enzymatic reaction.[42,45] Thus, the involvement of bis(μ-oxo) species in the aromatic hydroxylation reaction remains to be examined in more detail.

We gratefully acknowledge the contributions of our co-workers listed in the reference papers. We also thank the Ministry of Education, Culture, Sports, Science and Technology, Japan, for the continuous support.

References

(1) Itoh, S. Dicopper enzymes. In *Comprehensive Coordination Chemistry II*; Que, L., Jr., Tolman, W. B., Eds.; Elsevier: Amsterdam, 2004; Vol. 8, pp 369–393.

(2) Halcrow, M. A.; Knowles, P. F.; Phillips, S. E. V. Copper proteins in the transport and activation of dioxygen, and the reduction of inorganic molecules. In *Handbook on Metalloproteins*; Bertini, I., Sigel, A., Sigel, H., Eds.; Marcel Dekker, Inc.: New York, 2001; pp 709–762.

(3) (a) Matoba, Y.; Kumagai, T.; Yamamoto, A.; Yoshitsu, H.; Sugiyama, M. Crystallographic evidence that the dinuclear copper center of tyrosinase is flexible during catalysis. *J. Biol. Chem.* **2006**, *281*, 8981–8990. (b) Decker, H.; Schweikardt, T.; Tuczek, F. The first crystal structure of tyrosinase: All questions answered. *Angew. Chem., Int. Ed.* **2006**, *45*, 4546–4550.

(4) (a) Klabunde, T.; Eicken, C.; Sacchettini, J. C.; Krebs, B. Crystal structure of a plant catechol oxidase containing a dicopper center. *Nat. Struct. Biol.* **1998**, *5*, 1084–1090. (b) Gerdemann, C.; Eicken, C.; Krebs, B. The crystal structure of catechol oxidase: New insight into the function of type-3 copper proteins. *Acc. Chem. Res.* **2002**, *35*, 183–191.

(5) (a) Magnus, K. A.; Hazes, B.; Ton-That, H.; Bonaventura, C.; Bonaventura, J.; Hol, W. G. J. Crystallographic analysis of oxygenated and deoxygenated states of arthropod hemocyanin shows unusual differences. *Proteins* **1994**, *19*, 302–309. (b) Cuff, M. E.; Miller, K. I.; van Holde, K. E.; Hendrickson, W. A. Crystal structure of a functional unit from octopus hemocyanin. *J. Mol. Biol.* **1998**, *278*, 855–870.

(6) Sánchez-Ferrer, Á.; Rodríguez-López, J. N.; García-Cánovas, F.; García-Carmona, F. Tyrosinase: A comprehensive review of its mechanism. *Biochim. Biophys. Acta* **1995**, *1274*, 1–11.

(7) Turano, P.; Lu, Y. Iron in heme and related proteins. In *Handbook on Metalloproteins*; Bertini, I., Sigel, A., Sigel, H., Eds.; Marcel Dekker, Inc.: New York, 2001; pp 269–356.

(8) Solomon, E. I.; Sundaram, U. M.; Machonkin, T. E. Multicopper oxidases and oxygenases. *Chem. Rev.* **1996**, *96*, 2563–2605.

(9) (a) Kitajima, N.; Fujisawa, K.; Moro-oka, Y. μ-η^2:η^2-Peroxo binuclear copper complex, $[Cu(HB(3,5\text{-}iPr_2pz)_3)]_2(O_2)$. *J. Am. Chem. Soc.* **1989**, *111*, 8975–8976. (b) Kitajima, N.; Fujisawa, K.; Fujimoto, C.; Moro-oka, Y.; Hashimoto, S.; Kitagawa, T.; Toriumi, K.; Tatsumi, K.; Nakamura, A. A new model for dioxygen binding in hemocyanin. Synthesis, characterization, and molecular structure of the μ-η^2:η^2-peroxo dinuclear copper(II) complexes, $[Cu(HB(3,5\text{-}R_2pz)_3)]_2(O_2)$ (R = i-Pr and Ph). *J. Am. Chem. Soc.* **1992**, *114*, 1277–1291.

(10) Blackburn, N. J.; Strange, R. W.; Farooq, A.; Haka, M. S.; Karlin, K. D. X-ray absorption studies of three-coordinate dicopper(I) complexes and their dioxygen adducts. *J. Am. Chem. Soc.* **1988**, *110*, 4263–4272.

(11) Mirica, L. M.; Ottenwaelder, X.; Stack, T. D. P. Structure and spectroscopy of copper-dioxygen complexes. *Chem. Rev.* **2004**, *104*, 1013–1045.

(12) Lewis, E. A.; Tolman, W. B. Reactivity of dioxygen-copper systems. *Chem. Rev.* **2004**, *104*, 1047–1076.

(13) Hatcher, L. Q.; Karlin, K. D. Ligand influences in copper-dioxygen complex-formation and substrate oxidations. *Adv. Inorg. Chem.* **2006**, *58*, 131–184.

(14) Itoh, S.; Tachi, Y. Structure and O_2-reactivity of copper(I) complexes supported by pyridylalkylamine ligands. *Dalton Trans.* **2006**, 4531–4538.

(15) (a) Kitajima, N.; Koda, T.; Iwata, Y.; Moro-oka, Y. Reaction aspects of a μ-peroxo binuclear copper(II) complex. *J. Am. Chem. Soc.* **1990**, *112*, 8833–8839. (b) Paul, P. P.; Tyeklár, Z.; Jacobson, R. R.; Karlin, K. D. Reactivity patterns and comparisons in three classes of synthetic copper-dioxygen $\{Cu_2\text{-}O_2\}$ complexes: Implication for structure and biological relevance. *J. Am. Chem. Soc.* **1991**, *113*, 5322–5332. (c) Obias, H. V.; Lin, Y.; Murthy, N. N.; Pidcock, E.; Solomon, E. I.; Ralle, M.; Blackburn, N. J.; Neuhold, Y.-M.; Zuberbühler, A. D.; Karlin, K. D. Peroxo-, oxo-, and hydroxo-bridged dicopper complexes: Observation of exogenous hydrocarbon substrate oxidation. *J. Am. Chem. Soc.* **1998**, *120*, 12960–12961. (d) Mahapatra, S.; Halfen, J. A.; Wilkinson, E. C., Jr.; Tolman, W. B. Modeling copper-dioxygen reactivity in proteins: Aliphatic C-H bond activation by a new dicopper(II)-peroxo complex. *J. Am. Chem. Soc.* **1994**, *116*, 9785–9786. (e) Halfen, J. A.; Young, V. G., Jr.; Tolman, W. B. An unusual ligand oxidation by a (μ-η^2:η^2-peroxo)dicopper compound: 1° > 3° C-H bond selectivity and a novel bis(μ-alkylperoxo)dicopper intermediate. *Inorg. Chem.* **1998**, *37*, 2102–2103. (f) Mahadevan, V.; DuBois, J. L.; Hedman, B.; Hodgson, K. O.; Stack, T. D. P. Exogenous substrate reactivity with a $[Cu(III)_2O_2]^{2+}$ core: Structural implications. *J. Am. Chem. Soc.* **1999**, *121*, 5583–5584. (g) Mahadevan, V.; Henson, M. J.; Solomon, E. I.; Stack, T. D. P. Differential reactivity between interconvertible side-on peroxo and bis-μ-oxodicopper isomers using peralkylated diamine ligands. *J. Am. Chem. Soc.* **2000**, *122*, 10249–10250.

(16) Osako, T.; Ohkubo, K.; Taki, M.; Tachi, Y.; Fukuzumi, S.; Itoh, S. Oxidation mechanism of phenols by dicopper-dioxygen (Cu_2/O_2) complexes. *J. Am. Chem. Soc.* **2003**, *125*, 11027–11033.

(17) Itoh, S.; Nakao, H.; Berreau, L. M.; Kondo, T.; Komatsu, M.; Fukuzumi, S. Mechanistic studies of aliphatic ligand hydroxylation of a copper complex by dioxygen: A model reaction for copper monooxygenases. *J. Am. Chem. Soc.* **1998**, *120*, 2890–2899.

(18) Itoh, S.; Taki, M.; Nakao, H.; Holland, P. L.; Tolman, W. B.; Que, L., Jr.; Fukuzumi, S. Aliphatic hydroxylation by a bis(μ-oxo)dicopper(III) complex. *Angew. Chem., Int. Ed.* **2000**, *39*, 398–400.
(19) Marcus, R. A.; Sutin, N. Electron transfer in chemistry and biology. *Biochim. Biophys. Acta* **1985**, *811*, 265–322.
(20) Gardner, K. A.; Kuehnert, L. L.; Mayer, J. M. Hydrogen atom abstraction by permanganate: Oxidations of arylalkanes in organic solvents. *Inorg. Chem.* **1997**, *36*, 2069–2078.
(21) Weatherly, S. C.; Yang, I. V.; Thorp, H. H. Proton-coupled electron transfer in duplex DNA: Driving force dependence and isotope effects on electrocatalytic oxidation of guanine. *J. Am. Chem. Soc.* **2001**, *123*, 1236–1237.
(22) Mayer, J. M.; Hrovat, D. A.; Thomas, J. L.; Borden, W. T. Proton-coupled electron transfer versus hydrogen atom transfer in benzyl/toluene, methoxyl/methanol, and phenoxyl/phenol self-exchange reactions. *J. Am. Chem. Soc.* **2002**, *124*, 11142–11147.
(23) Fukuzumi, S.; Shimoosako, K.; Suenobu, T.; Watanabe, Y. Mechanisms of hydrogen-, oxygen-, and electron-transfer reactions of cumylperoxyl radical. *J. Am. Chem. Soc.* **2003**, *125*, 9074–9082.
(24) Pidcock, E.; DeBeer, S.; Obias, H. V.; Hedman, B.; Hodgson, K. O.; Karlin, K. D.; Solomon, E. I. A study of solid $[\{Cu(MePY2)\}_2O_2]^{2+}$ using resonance Raman and X-ray absorption spectroscopies: An intermediate Cu_2O_2 core structure or a solid solution. *J. Am. Chem. Soc.* **1999**, *121*, 1870–1878.
(25) (a) Santagostini, L.; Gullotti, M.; Monzani, E.; Casella, L.; Dillinger, R.; Tuczek, F. Reversible dioxygen binding and phenol oxygenation in a tyrosinase model system. *Chem.—Eur. J.* **2000**, *6*, 519–522. (b) Palavicini, S.; Granata, A.; Monzani, E.; Casella, L. Hydroxylation of phenolic compounds by a peroxodicopper(II) complex: Further insight into the mechanism of tyrosinase. *J. Am. Chem. Soc.* **2005**, *127*, 18031–18036.
(26) Itoh, S.; Kumei, H.; Taki, M.; Nagatomo, S.; Kitagawa, T.; Fukuzumi, S. Oxygenation of phenols to catechols by a (μ-η^2:η^2-peroxo)dicopper(II) complex. Mechanistic insight into the phenolase activity of tyrosinase. *J. Am. Chem. Soc.* **2001**, *123*, 6708–6709.
(27) (a) Karlin, K. D.; Dahlstrom, P. L.; Cozzette, S. N.; Scensny, P. M.; Zubieta, J. Activation of O_2 by a binuclear copper(I) compound. Hydroxylation of a new xylyl-binucleating ligand to produce a phenoxyl-bridged binuclear copper(II) complex: X-ray crystal structure of $[Cu_2\{OC_6H_3[CH_2N(CH_2CH_2py)_2]_2\text{-}2,6\}(OMe)]$ (py = 2-pyridyl). *J. Chem. Soc., Chem. Commun.* **1981**, 881–882. (b) Karlin, K. D.; Gultneh, Y.; Hutchinson, J. P.; Zubieta, J. Three-coordinate binuclear copper(I) complex: Model compound for the copper sites in deoxyhemocyanin and deoxytyrosinase. *J. Am. Chem. Soc.* **1982**, *104*, 5240–5242. (c) Karlin, K. D.; Hayes, J. C.; Gultneh, Y.; Cruse, R. W.; McKown, J. W.; Hutchinson, J. P.; Zubieta, J. Copper-mediated hydroxylation of an arene: Model system for the action of copper monooxygenases. Structures of a binuclear Cu(I) complex and its oxygenated product. *J. Am. Chem. Soc.* **1984**, *106*, 2121–2128.
(28) Yamazaki, S.; Itoh, S. Kinetic evaluation of phenolase activity of tyrosinase using simplified catalytic reaction system. *J. Am. Chem. Soc.* **2003**, *125*, 13034–13035.
(29) James, T. D.; Sandanayake, K. R. A. S.; Shinkai, S. Recognition of sugars and related compounds by "reading-out"-type interfaces. *Supramol. Chem.* **1995**, *6*, 141–157.
(30) Decker and co-workers pointed out that His194 forms a π–π stacking interaction with Tyr98 of the caddie protein.[3b] Thus, His194 could also be regarded as the base. No basic residue other than the histidine copper ligands has been identified around the active site pocket of tyrosinase (within ~8 Å of the Cu_2O_2 core).[3a]
(31) van Holde, K. E.; Miller, K. I.; Decker, H. Hemocyanins and invertebrate evolution. *J. Biol. Chem.* **2001**, *276*, 15563–15566.
(32) Magnus, K. A.; Ton-That, H.; Carpenter, J. E. Recent structural work on the oxygen transport protein hemocyanin. *Chem. Rev.* **1994**, *94*, 727–735.
(33) Jaenicke, E.; Decker, H. Functional changes in the family of type 3 copper proteins during evolution. *ChemBioChem* **2004**, *5*, 163–169.
(34) Miller, K. I.; Schabtach, E.; van Holde, K. E. Arrangement of subunits and domains within the *Octpus dofleini* hemocyanin molecule. *Proc. Acad. Natl. Sci. U.S.A.* **1990**, *87*, 1496–1500.
(35) Zlateva, T.; Di Muro, P.; Salvato, B.; Beltramini, M. The *o*-diphenol oxidase activity of arthropod hemocyanin. *FEBS Lett.* **1996**, *384*, 251–254.
(36) Decker, H.; Rimke, T. Tarantula hemocyanin shows phenoloxidase activity. *J. Biol. Chem.* **1998**, *273*, 25889–25892.
(37) Lee, S. Y.; Lee, B. L.; Söderhäll, K. Processing of crayfish hemocyanin subunits into phenoloxidase. *Biochem. Biophys. Res. Commun.* **2004**, *322*, 490–496.
(38) Nagai, T.; Osaki, T.; Kawata, S. Functional conversion of hemocyanin to phenoloxidase by horseshoe crab antimicrobial peptides. *J. Biol. Chem.* **2001**, *276*, 27166–27170.
(39) Salvato, B.; Santamaria, M.; Beltramini, M.; Alzuet, G.; Casella, L. The enzymatic properties of *Octopus vulgaris* hemocyanin: *o*-Diphenol oxidase activity. *Biochemistry* **1998**, *37*, 14065–14077.
(40) Morioka, C.; Tachi, Y.; Suzuki, S.; Itoh, S. Significant enhancement of monooxygenase activity of oxygen carrier protein hemocyanin by urea. *J. Am. Chem. Soc.* **2006**, *128*, 6788–6789.
(41) It was reported that the treatment of octopus hemocyanin with a high concentration of urea induced dissociation of the subunits from a native supramolecular assembly of hemocyanin: Salvato, B.; Ghiretti-Magaldi, A.; Ghiretti, F. Hemocyanin of *Octopus vulgaris*. The molecular weight of the minimal functional subunit in 3 M urea. *Biochemistry* **1979**, *18*, 2731–2736.
(42) The DFT study by Siegbahn has suggested that the phenolic proton of the substrate is abstracted by the bridging hydroxyl group of Cu^I–OH–Cu^I moiety of deoxy-tyrosinase. In this case, however, binding of O_2 to deoxy-tyrosinase occurs after substrate binding to give a (μ-η^1:η^1-superoxo)dicopper(I,II) active species, which is totally different from the generally accepted active oxygen species **A**: Siegbahn, P. E. M. The catalytic cycle of tyrosinase: Peroxide attack on the phenolate ring followed by O–O bond cleavage. *J. Biol. Inorg. Chem.* **2003**, *8*, 567–576.
(43) Mirica, L. M.; Vance, M.; Rudd, D. J.; Hedman, B.; Hodgson, K. O.; Solomon, E. I.; Stack, T. D. P. Tyrosinase reactivity in a model complex: An alternative hydroxylation mechanism. *Science* **2005**, *308*, 1980–1892.
(44) Itoh, S.; Bandoh, H.; Nakagawa, M.; Nagatomo, S.; Kitagawa, T.; Karlin, K. D.; Fukuzumi, S. Formation, characterization, and reactivity of bis(μ-oxo)dinickel(III) complexes supported by a series of bis[2-(2-pyridyl)ethyl]amine ligands. *J. Am. Chem. Soc.* **2001**, *123*, 11168–11178.
(45) Siegbahn, P. E. M.; Wirstam, M. Is the bis-μ-oxo Cu_2(III,III) state an intermediate in tyrosinase? *J. Am. Chem. Soc.* **2001**, *123*, 11819–11820.

AR6000395